AD_____
(Leave blank)

Award Number:
W81XWH-10-1-0188

TITLE:
Improved Assessments of Breast Cancer Therapies with DCE-MRI

PRINCIPAL INVESTIGATOR:
Julio C. Cárdenas

CONTRACTING ORGANIZATION:
University of Arizona
Tucson, AZ 85724

REPORT DATE:
April 2011

TYPE OF REPORT:
Annual Summary

PREPARED FOR:
U.S. Army Medical Research and Materiel Command
Fort Detrick, Maryland 21702-5012

DISTRIBUTION STATEMENT: (Check one)

Approved for public release; distribution unlimited

REPORT DOCUMENTATION PAGE

Form Approved
OMB No. 0704-0188

1. REPORT DATE *(DD-MM-YYYY)*	2. REPORT TYPE	3. DATES COVERED *(From - To)*
1 April 2011	Annual Summary	1 Apr 2010 – 31 Mar 2011

4. TITLE AND SUBTITLE

Improved Assessments of Breast Cancer Therapies with DCE-MRI

5a. CONTRACT NUMBER

5b. GRANT NUMBER
W81XWH-10-1-0188

5c. PROGRAM ELEMENT NUMBER

6. AUTHOR(S)

Julio C. Cárdenas

cardenaj@email.arizona.edu

5d. PROJECT NUMBER

5e. TASK NUMBER

5f. WORK UNIT NUMBER

7. PERFORMING ORGANIZATION NAME(S) AND ADDRESS(ES)

University of Arizona
Arizona Cancer Center
Tucson, AZ 85724

8. PERFORMING ORGANIZATION REPORT NUMBER

9. SPONSORING / MONITORING AGENCY NAME(S) AND ADDRESS(ES)

U.S. Army Medical Research
Fort Detrick, Maryland
21702-5012

10. SPONSOR/MONITOR'S ACRONYM(S)

11. SPONSOR/MONITOR'S REPORT NUMBER(S)

12. DISTRIBUTION / AVAILABILITY STATEMENT

Approved for public release; distribution unlimited

13. SUPPLEMENTARY NOTES

14. ABSTRACT

Dynamic Contrast Enhancement MRI (DCE MRI) has been used in clinical and pre-clinical trials of anti-angiogenic breast cancer therapies, but its high variability severely reduces the value of this imaging modality to asses the early response to anti-angiogenic therapies in an individual patient. Since the start of this grant we have developed a new pharmacokinetic model for DCE-MRI that removes the effect of hematocrit and blood flow on relative measurement of tumor permeability. The only inputs required by this model are the concentration of two tracers in the tumor vasculature as a function of time. This is an improvement over previous reference-region models that require estimates of the tissue permeability and distribution to volume of one of the agents in addition to the absolute concentration of both agents. An important assumption in this model is that both tracers are detected simultaneously within the tissue of interest; in order to accomplish such task we designed and synthesized a new series of ^{19}F-MRI contrast agents that can be selectively detected within the same region of interest. We also optimized our ^{19}F-DCE-MRI protocol to obtain images of ^{19}F contrast agents with the same temporal resolutions than standard ^{1}H-DCE-MRI. Finally, we were also able to collect ^{19}F images one of the agents in a mouse model of breast cancer with high temporal resolution for such studies.

15. SUBJECT TERMS

Breast Cancer , DCE-MRI, Fluorine-19 MRI, Pharmacokinetics

16. SECURITY CLASSIFICATION OF:			17. LIMITATION OF ABSTRACT	18. NUMBER OF PAGES	19a. NAME OF RESPONSIBLE PERSON
					USAMRMC
a. REPORT	b. ABSTRACT	c. THIS PAGE	UU	10	19b. TELEPHONE NUMBER *(include area code)*
U	U	U			

Standard Form 298 (Rev. 8-98)
Prescribed by ANSI Std. Z39.18

Table of Contents

A. Introduction

Angiogenesis is critical for the sustained growth[1,2] and metastasis[3] of solid tumors. Anti-angiogenic therapies are often cytostatic (do not decrease tumor volume), so that evaluations of vascular permeabilities and fractional blood volumes are required to assess early therapeutic responses.[4] Dynamic Contrast Enhanced MRI (DCE MRI) has been used to detect changes in vascular permeability, typically represented by the parameter Ktrans, by monitoring the rate of uptake and/or wash-out of a T1 MRI contrast agent in the tumor tissue. The results from many DCE-MRI studies are correlated with microvessel densities,[5] expression of VEGF[6] and other measurements of tumor viability. Although DCE MRI can provide semi-quantitative results in preclinical studies, the high variability of the DCE MRI measurements of Ktrans can only produce marginal, qualitative assessments of tumor angiogenesis in the clinic.[7] Our central hypothesis is that variations of hematocrit and blood flow between patients are the primary sources of the variability in DCE MRI measurements of vascular permeability. We proposed a new reference-region model for DCE-MRI that will improve the assessment of anti-angiogenic breast cancer therapies by removing the effects of variations in the hematocrit and blood flow within the tumor microvasculature.

B. Key Accomplishments

B1. Training Accomplishments

General Training

During the first year of this project I completed all my course work and was advanced to PhD candidacy by the Department of Chemistry at the University of Arizona. I continued my training on Magnetic Resonance Imaging under the mentorship of Dr. Mark D. Pagel (my advisor). I also completed and advance course in biostatistics, which has proven fundamental for the analysis and interpretation of some of the results reported here. All the courses I have taken and my cumulative GPD are listed in appendix one.

Project-specific Training

I collaborated with Dr. Pagel and Dr. Amanda Baker (Arizona Cancer Center) on the design, preparation and implementation of a study to asses the response of pancreatic tumors to a hypoxia-activated drug (TH-302) by DCE-MRI and Diffusion-Weighted MRI (DW-MRI). The spefici deliverables of this collaboration are: 1) A computer code written in Matlab to analyze T1-weighted DCE-MRI data using the model by Tofts et al. 2) I became proficient in the design and implementations of imaging protocols for T1 and T2-weighted MRI. 3) An specific protocol for the analysis of variations in K_{trans} using non-parametric and parametric hypothesis testing.

B2. Research Accomplishments

B2.1 DCE-MRI and DW-MRI to evaluate the effect of a hypoxia-activated chemotherapy

We used DCE-MRI and DW-MRI to investigate the biological response to TH-302, a hypoxia-activated prodrug in a pre-clinical model of pancreatic cancer. As a consequence of TH-302 selective effects on poorly-vascularized tumor regions, we expected a change in DCE-MRI and/or DW-MRI. The results showed that TH-302 caused a change in tumor vasculature as measured with DCE-MRI, but did not change cell membrane integrity measured with DW-MRI. These effects were homogenous throughout the tumor. These results demonstrate advantages of combining DCE-MRI and DW-MRI for therapy studies. (Figures 1 and 2).

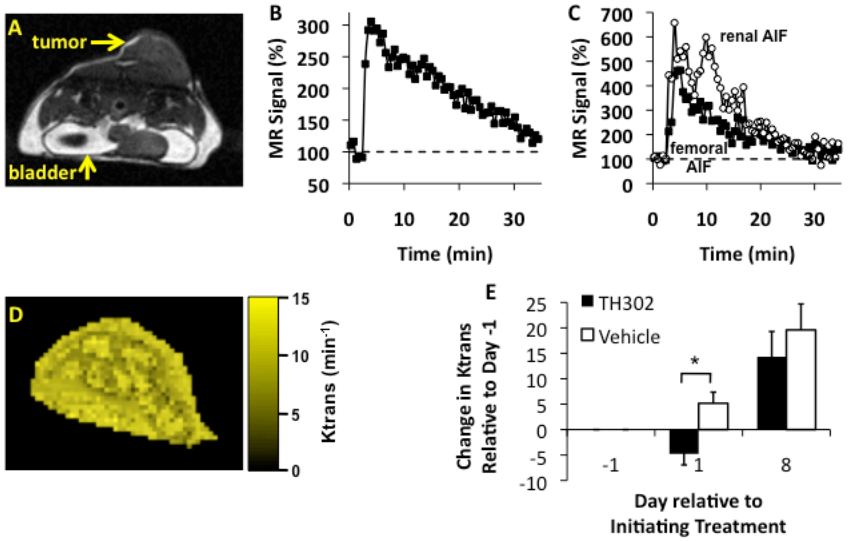

Figure 1. The effect of TH-302 therapy on Ktrans measured with DCE-MRI.

A) An anatomical image shows the location of the tumor. Dark bands below the tumor were caused by excitation of orthogonal slices that imaged the renal artery. B) After injecting the agent, a strong change in MRI signal was observed in the tumor. C) The Arterial Input Function (AIF) from the femoral artery showed less variability than the renal AIF. D) The parametric map of Ktrans values showed good spatial homogeneity. E) The relative median Ktrans decreased on Day 1 following TH-302 therapy while Ktrans increased with vehicle treatment. (The height shows the median for each Bars indicate medians, Error bars represent standard deviations; * indicates $p < 0.05$ for the null hypothesis of groups with equal medians.

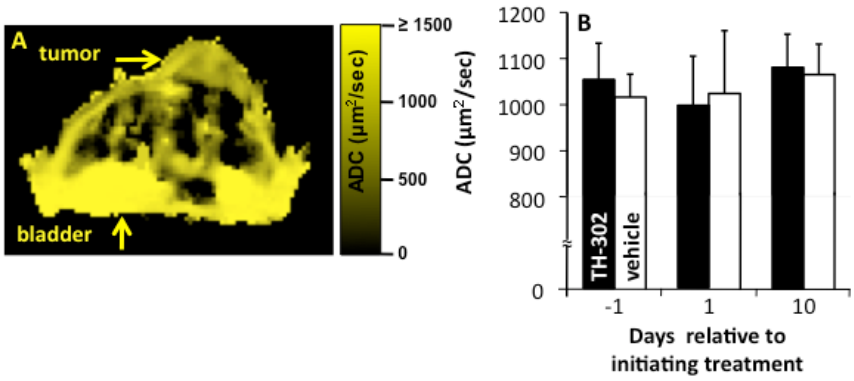

Figure 2. The effect of TH-302 therapy on ADC measured with DW-MRI.

A) The parametric map of ADC values showed good spatial homogeneity, especially relative to the torso. The anatomical image that corresponds to this ADC map is shown in Figure 2A. B) The average ADC did not change following TH-302 therapy. Error bars represent the standard deviation of cohorts 7 mice. All average ADC values were statistically equivalent ($p > 0.05$ for all 15 pairs of the 6 values).

B2.1 Derivation of a new reference-region model for DCE-MRI

Since the start of this grant we have developed a new pharmacokinetic model for DCE-MRI that removes the effect of hematocrit and blood flow on relative measurement of tumor permeability. The only inputs required by this model are the concentration of two tracers in the tumor vasculature as a function of time. This is an improvement over previous reference-region models that require estimates of the tissue permeability and distribution volume of one of the agents in addition to the absolute concentration of both agents.(Yankeelov). The derivation of the final equation that will be used to analyze all the DCE-MRI data is described in Figure 3.

The differential equations for each agent are:

$$\frac{dC_{T1}}{dt} = K^{trans1} * C_{p1(t)} - \frac{K^{trans1}}{Ve_1} C_{T1} \quad (1)$$

$$\frac{dC_{T2}}{dt} = K^{trans2} * C_{p2(t)} - \frac{K^{trans2}}{Ve_2} C_{T2} \quad (2)$$

From equation (2)

$$C_{p2(t)} = \frac{1}{K^{trans2}} * \frac{dC_{T2}}{dt} + \frac{1}{Ve_2} * C_{T2} \quad (3)$$

if $C_{p1(t)} = C_{p2(t)}$ and substituting eq(3) in eq(1), we get:

$$\frac{dC_{T1}}{dt} = K^{trans1} * \left[\frac{1}{K^{trans2}} * \frac{dC_{T2}}{dt} + \frac{1}{Ve_2} * C_{T2} \right] - \frac{K^{trans1}}{Ve_1} C_{T1}$$

$$\frac{dC_{T1}}{dt} = \frac{K^{trans1}}{K^{trans2}} * \frac{dC_{T2}}{dt} + \frac{K^{trans1}}{Ve_2} * C_{T2} - \frac{K^{trans1}}{Ve_1} C_{T1} \quad (4a)$$

if $Ve_1 = Ve_2$, and $R^{Ktrans} = \frac{K^{trans1}}{K^{trans2}}$, equation 4a becomes:

$$\frac{dC_{T1}}{dt} = R^{Ktrans} * \frac{dC_{T2}}{dt} + kep_1 * C_{T2} - kep_1 * C_{T1} \quad (4b)$$

Integrating on both sides and multiplying by dt, we get

$$\int dC_{T1} = R^{Ktrans} \int dC_{T2} + kep_1 * \left[\int C_{T2} dt - \int C_{T1} dt \right] + C$$

Applying the initial the conditions $C_{T1} = C_{T2} = 0$ at $t = 0$, we get:

$$C_{T1(t)} = R_{Ktrans} * C_{T2(t)} + Kep_1 \left[\int_0^t C_{T2(t)}\, dt - \int_0^t C_{T1(t)}\, dt \right]$$

Aproximating the integrals using summations:

$$C_{T1(t)} \approx R_{Ktrans} * C_{T2(t)} + Kep_1 \left[\sum_0^t C_{T2(t)} \Delta t - \sum_0^t C_{T1(t)} \Delta t \right] \quad (5)$$

Equation (5) can be fitted by multiple linear regression to obtain R_{Ktrans} and Kep_1

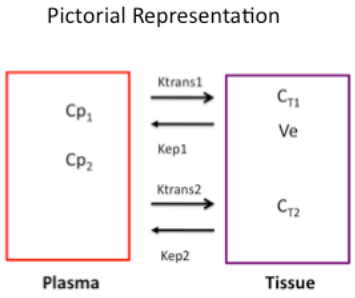

Figure 3. Derivation of a new equation to calculate relative K_{trans} and k_{ep} for two tracers

According to computer simulations performed with this new model, it is possible to calculate the relative permeability of two agents with an error of less than 0.5 % (Table 1).

		Calculated by New model	
Constant	**Expected**	**Ct=agent_one**	**Ct=agent_two**
K_{trans1} / K_{trans2}	0.217	0.217	NA
kep_1	0.0619	0.0619	NA
K_{trans2} / K_{trans1}	4.615	NA	4.606
kep_2	0.2857	NA	0.285

Table 1. Calculated and expected values of the pharmacokinetic parameters of the new model.

B2.1 Synthesis of a new class of contrast agents for 19F-DCE-MRI

An important assumption in this model is that both tracers are detected simultaneously within the tissue of interest; in order to accomplish such task we designed and synthesized a new series of derivatives of a new ^{19}F-MRI contrast agent that can be selectively detected within the same region of interest (Figure 4). The Larmor frequency of the CF3 groups in these molecules is changed by the presence of specific lanthanides in the chelating ring. Figure 5 shows how the selection of the lanthanide affects the resonance frequency of the CF3 group. All the compounds were characterized by Mass Spectrometry, and ^{13}C, ^{1}H, ^{19}F, NMR.

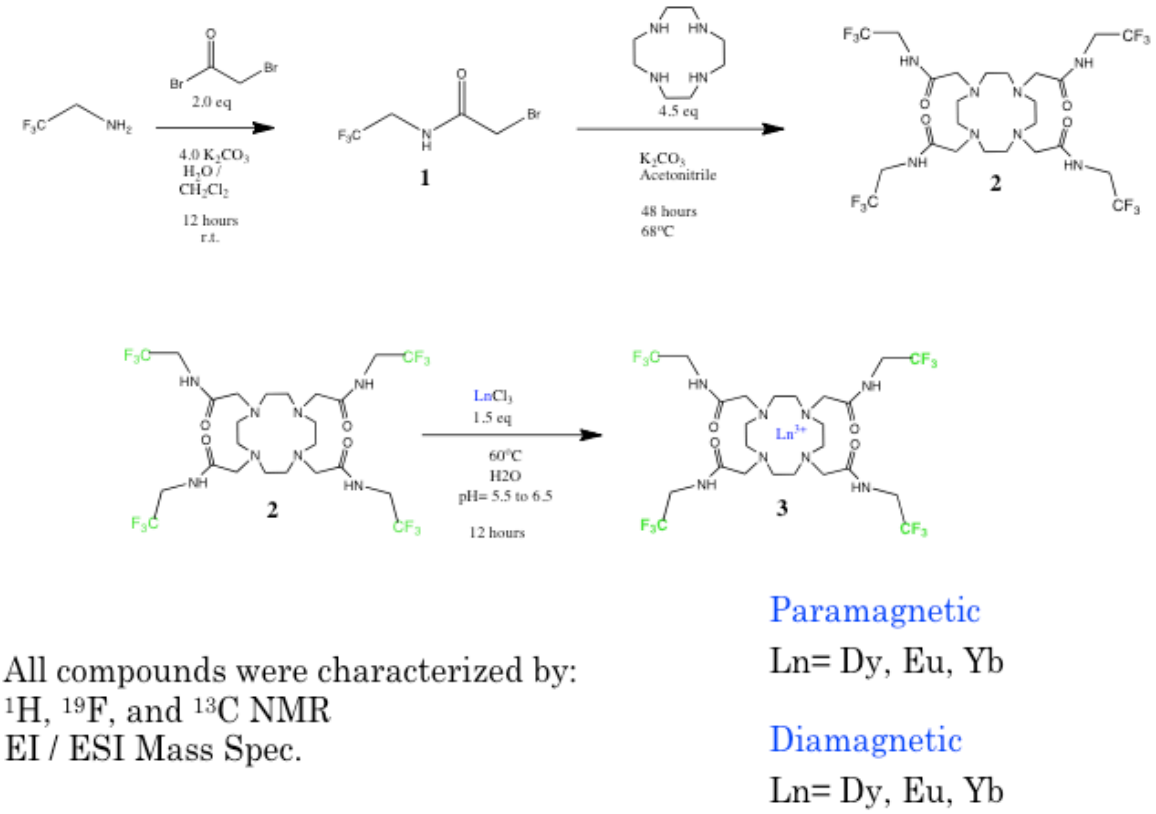

Figure 4. Synthesis of a new class of 19F-MRI contrast agents.

An advantage of ^{19}F-MRI over standard ^{1}H-MRI is that the correlation between the concentration and signal is linear, therefore is not necessary to know the T1-relaxivity of the tissue of interest before injection of the contrast agent. However, when we tried to collect images of these new compounds we realized that the concentration required to obtain images in reasonable amount of time is 20 times higher than the concentration obtained for a saturated solution of any of these compounds. Therefore, we decided to synthesize emulsions of perfluorinated-15-crown-ether and perfluoro-octane.

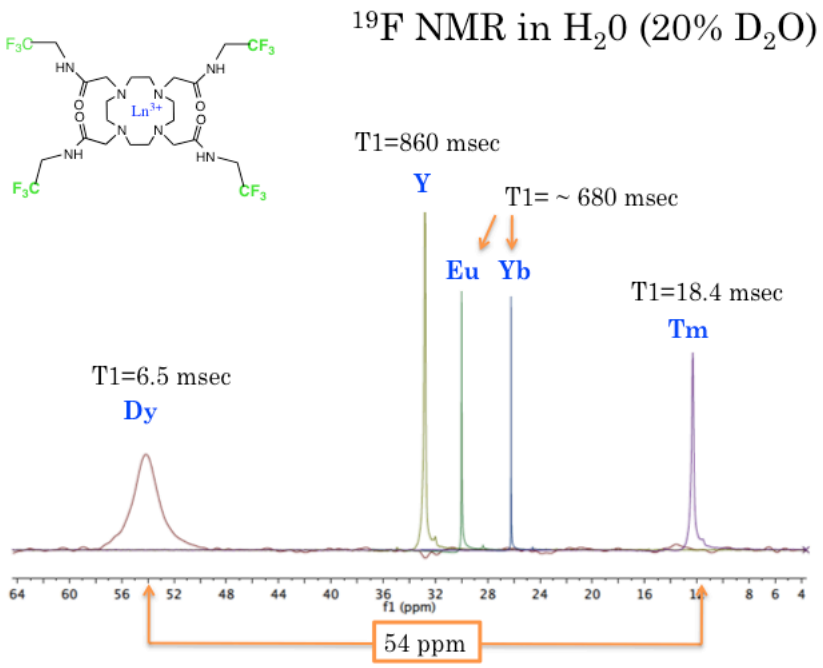

Figure 5. The effect on lanthanide selection on the Resonance Frequency of the CF3 group

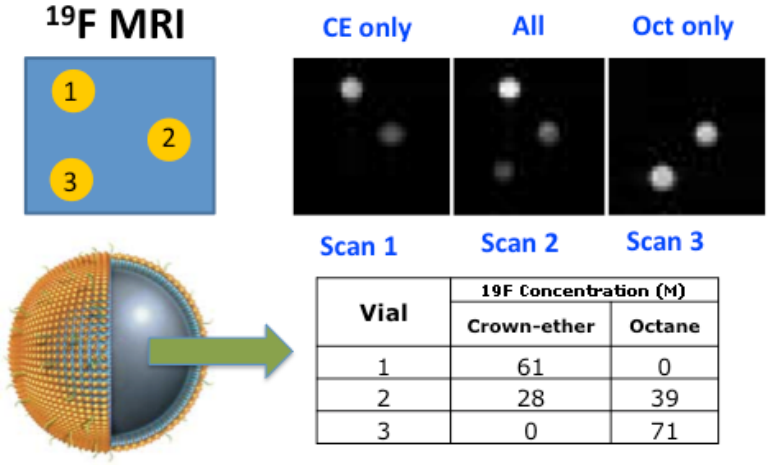

Vial	19F Concentration (M)	
	Crown-ether	Octane
1	61	0
2	28	39
3	0	71

Figure 6. Selective MRI of 19F nanoemulsions of perfluoro- 15-crown-ether and perfluoro-octane

With these new agents it is possible to reach a concentration of up to 71 Molar. Which is about 35 times higher than our limit of detection. Additionally, we were able to image a mixture of these agents selectively. The details are provided in Figure 6. We also optimized our ^{19}F-DCE-MRI protocol to obtain images of ^{19}F contrast agents with the same temporal resolutions than standard ^{1}H-DCE-MRI. Finally, we were also able to collect ^{19}F images one of the agents in a mouse model of breast cancer with high temporal resolution for such studies. (Figure 7).

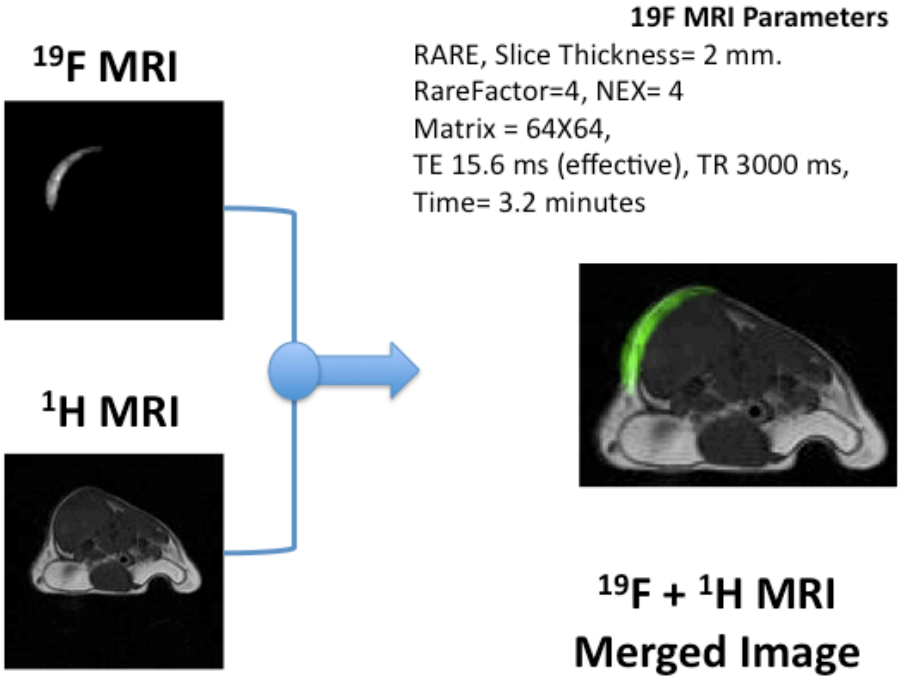

Figure 7. In vivo MRI of 19F a 60 nm emulsion of perfluoro- 15-crown-ether

C. Reportable Outcomes

Section B2.1 of this report will be presented as traditional poster during the 2011 meeting of International Society of Magnetic Resonance in Medicine in Montreal, Canada. A manuscript describing the results of this section will be prepared and submitted for publication. A manuscript about the results on section B2.2 is also under preparation.

D. Conclusion

We have developed a new reference-region model for DCE-MRI. We also designed and synthesized a new class of 19F-MRI contrast agents that can be detected in vivo. Our future work includes the simultaneous detection of two agents in vivo, and the analysis of their pharmacokinetics properties using our new DCE-MRI model.

E. References

1. Folkman J. Tumor angiogenesis: therapeutic implications. N Engl J Med, 1971, 285:1182-1186.
2. Folkman J, Watson K, Ingber D, Hanahan D. Induction of angiogenesis during the transition from hyperplasia to neoplasia. Nature, 1989, 339:58-61.
3. Weidner N, Semple JP, Welch WR, Folkman J. Tumor angiogenesis and metastasis – correlation in invasive breast carcinoma. N Engl J Med, 1991, 324:1-8.
4. Kaban K, Herbst RS. Angiogenesis as a target for cancer therapy. Hematol Oncol Clin North Am, 2002, 16:1125-1171.
5. Van Dijke CF, Brasch RC, Roberts TPL, Weidner N, Mathur A, Shames DM, Mann JS, Demsar F, Lang P, Schwickert HC. Mammary carcinoma model: correlation of macromolecular contrast-enhanced MR imaging characterizations of tumor microvasculature and histologic capillary density. Radiology, 1996, 198:813-818.
6. Ikeda O, Nishimura R, Miyayama H, Yasunaga T, Ozaki Y, Tuji A, Yamashita Y. Evaluation of tumor angiogenesis using dynamic enhanced magnetic resonance imaging: comparison of plasma vascular endothelial growth factor, hemodynamic, and pharmacokinetic parameters. Acta Radiologica, 2004, 45(4):446-452.
7. Padhani AR. Dynamic contrast-enhanced MRI in clinical oncology: current status and future directions. J Magn Reson Imaging, 2002, 16(4):407-422.